Future Journal of Pharmaceutical Sciences

RESEARCH Open Access

Computational virtual screening and structure-based design of some epidermal growth factor receptor inhibitors

Muhammad Tukur Ibrahim*, Adamu Uzairu, Sani Uba and Gideon Adamu Shallangwa

Abstract

Background: The foremost cause of cancer mortality worldwide was lung cancer. Lung cancer is divided into small cell lung cancer and non-small cell lung cancer (NSCLC). The latter is the main type of lung cancer that account for about 90% of the cancer issues and estimate about 25% of the cancer mortality each year in the world. Among the types of lung cancer with about 1.5 million patients and less than 20% survival rate is NSCLC. Overexpression of EGFR tyrosine kinase was recognized to be the cause of NSCLC. Therefore, there is a need to develop more EGFR inhibitors due to drug-resistance development by the mutation.

Result: Computational virtual screening on some epidermal growth factor receptor inhibitors ($EGFR^{L858R/T790M}$ inhibitors or NSCLC therapeutic agents) against their target protein (EGFR tyrosine kinase receptor pdb entry **3IKA**) was performed via molecular docking simulation and pharmacokinetics to identify hit compounds with a promising affinity toward their target. The hit compounds discovered were compound 22 with −9.8 kcal/mol, 24 with −9.7 kcal/mol, 17 with −9.7 kcal/mol, and 19 with −9.5 kcal/mol respectively. These lead compounds were further subjected to drug-likeness and ADME prediction and found to be orally bioavailable. Six (6) new $EGFR^{L858R/T790M}$ inhibitors using compound 22 with the highest binding affinity as a template were designed.

Conclusion: The six newly $EGFR^{L858R/T790M}$ inhibitors were found to have a better binding affinity than the template used in the designing process and AZD9291 (the positive control). None of the designed compounds was found to violate more than the permissible limit set by RO5 thereby predicting their easy transportation, absorption, and diffusion. More so, the designed compounds were found to have good synthetic accessibility which indicates that these designed compounds can be easily synthesized in the laboratory.

Keywords: Computational, Docking, $EGFR^{L858R/T790M}$, Inhibitors, ADME, Drug-likeness

Background

Lung cancer is one of the leading cancer problems in the globe. It was reported to cause a lot of death every year (estimated to take about one-third of the entire cancer deaths). Non-small cell lung cancer (NSCLC) is the main subset of lung cancers that accounts for about 85% of the cancer problems [1]. Overexpression of epidermal growth factor receptor kinase was identified to be the common cause of NSCLCs. Report on NSCLCs on the population of patients in the Caucasia rise to about 10–15% and 30–40% in Asia [1].

The discovery of NSCLC therapeutic agents for the treatment of EGFR tyrosine kinase is one of the major challenges encountered by the medicinal chemist [2]. The treatment of EGFR tyrosine kinase to managed NSCLCs became a very urgent therapeutic necessity [3].

NSCLC therapeutic agents show a very high response rate in patients with arousing modifications of EGFR. NSCLC therapeutic agents or EGFR inhibitors are classified into reversible EGFR inhibitors (first-generation EGFR inhibitors); gefitinib and erlotinib are the example of this class of EGFR

* Correspondence: muhdtk1988@gmail.com
Department of Chemistry, Faculty of Physical Science, Ahmadu Bello University, P.M.B 1045, Zaria, Kaduna State, Nigeria

Table 1 The Structures of the data set

S/No	Structure	S/No	Structure
1	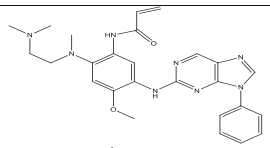	15	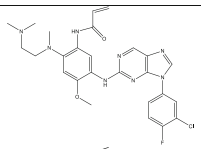
2	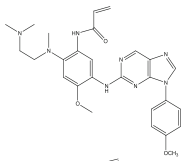	16	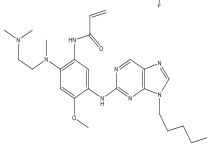
3	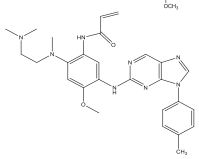	17	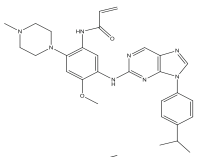
4	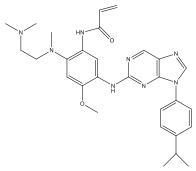	18	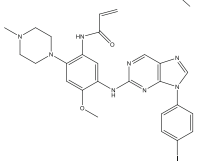
5	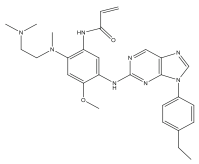	19	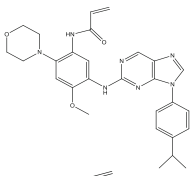
6	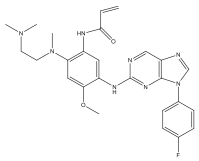	20	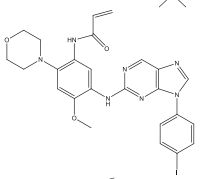
7	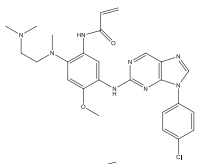	21	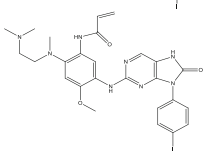
8	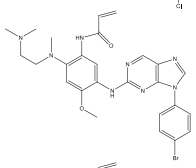	22	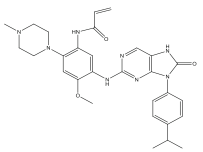
9	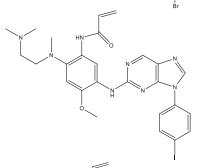	23	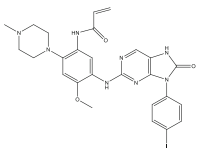
10	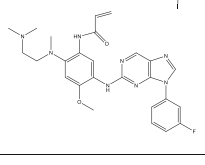	24	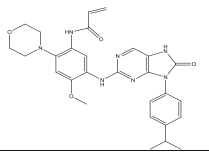

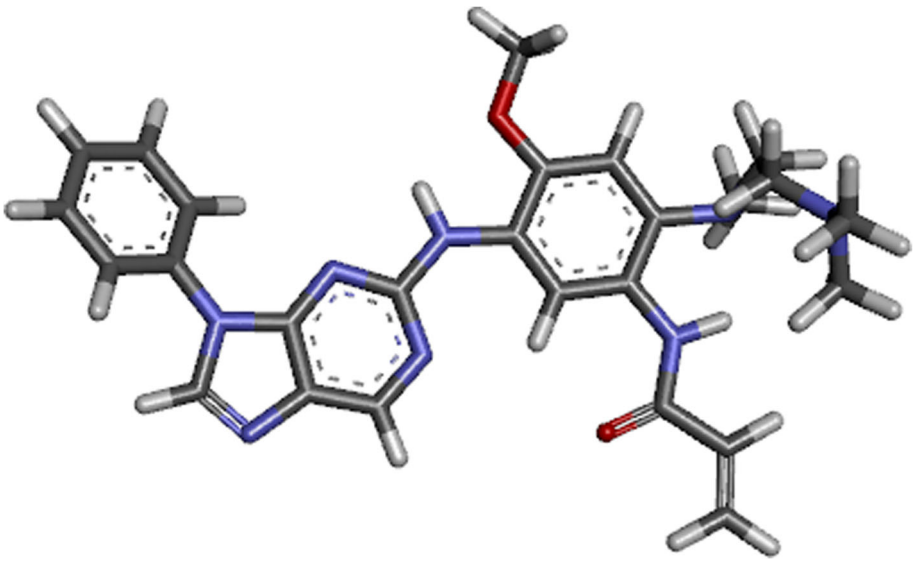

Fig. 1 3D geometry of a prepared $EGFR^{L858R/T790M}$ inhibitor (ligand)

inhibitors include. Unluckily, the span of the potency of these first-generation EGFR inhibitors is narrowed due to the development of drug resistance by the secondary mutation T790M [4]. And the irreversible EGFR inhibitors (second- and third-generation EGFR inhibitors), afatinib and osimertinib, are the examples of these EGFR inhibitors. Inline to defeat the resistance to the first-generation of EGFR inhibitors, the second-generation irreversible EGFR inhibitors, such as afatinib and canertinib, were afterward devised to treat NSCLC EGFR T790M mutation [5]. Yet, due to severe side effects, such as skin rash and diarrhea, these second-generation inhibitors cannot attain satisfaction over the first-generation reversible inhibitors. It is believed that the activities upon wild-type EGFR will narrow the possible activities on the patients with the T790M mutation [2, 6–8].

To approach the unmet clinical demands, many third-generation irreversible EGFR inhibitors, such as WZ-4002, rociletinib, olmutinib, and osimertinib were designed to inhibit the T790M resistance mutation while being more selective for wild type EGFR [2, 9–12].

Molecular docking is a molecular modeling technique used in structure-based design to screen a library of compounds to identify compounds with a higher affinity toward their target protein by elucidating their mode of interaction with their target utilizing their 3D structures [13]. Pharmacokinetics and drug-likeness properties prediction of hit compounds play a vital role in structure-based design in the determination of the pharmacokinetic profile of the hit compounds under investigation in the early stage of the drug pipeline [14].

This work is aimed at carrying out computational virtual screening on some $EGFR^{L858R/T790M}$ inhibitors using molecular docking to identify hit compounds with a promising affinity against their target receptor (EGFR tyrosine kinase receptor), confirm their bioavailability via their pharmacokinetics and drug-likeness properties, and design new potent $EGFR^{L858R/T790M}$ inhibitors that have better binding affinity than the template.

Method

This computational work was done on a Dell personal computer laptop, with these specifications: Intel ® Core™ i7 Dual CPU, M330 @2.75 GHz 2.75 GHz, and 8 GB of RAM. The following software was utilized to achieve the success of this research: Pyrex virtual screening software,

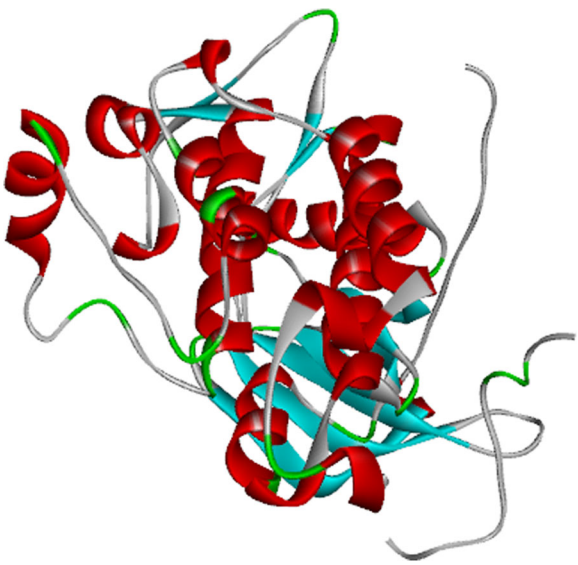

Fig. 2 3D structure of the prepared EGFR enzyme

Table 2 The interactions of the molecules under investigation in the active site of EGFR receptor

Complex	Binding affinity (Kcal/mol)	H Bond	Bond distance (Å)	Hydrophobic, electrostatic and Other Interactions
Complex 1	−8.2	LYS745 LYS875 GLY857 PHE723	2.4833 3.59309 3.72533 2.6702	ASP855, LEU718, PHE723 and LEU844
Complex 2	−8.0	ASP855 MET790 LYS745ASP855MET793GLY857PHE723	2.98309 2.54859 2.53945 3.28835 3.63827 3.69781 2.74564	ASP855, LEU718, PHE723 and LEU844
Complex 3	−8.3	LYS745ASN842ASP855ASP837GLY857 PHE723	2.55654 3.69674 3.46169 3.79142 3.5789 2.70142	ASP855, LEU718, PHE723, LEU718 and LEU844
Complex 4	−8.6	LYS745ASN842GLY857PHE723	2.57931 3.47241 3.71569 2.53735	ASP855, MET790, PHE723, LEU718(3), VAL726, ALA743 and LEU844 (2)
Complex 5	−8.4	MET790LYS745ASN842ASP855LYS875GLY857PHE723	2.63263 2.57166 3.5002 3.48749 3.7168 3.61079 2.69448	ASP855, LEU718 (2), PHE723, LEU792 and LEU844
Complex 6	−8.1	MET790ASP855LYS745LYS745 ASP855 GLY857	2.63344 2.45808 2.51691 2.75431 3.42724 3.68209	ASP855, LEU718, PHE723 and LEU844
Complex 7	−8.2	MET790LYS745ASN842GLY857PHE723	2.66828 2.50517 3.64733 3.71982 2.63929	ASP855, LEU718 (2), PHE723 and LEU844
Complex 8	−8.2	MET790LYS745ASP855LYS875GLY857PHE723	2.69124 2.49593 3.31777 3.56354 3.70766 2.66609	ASP855, PHE723, LEU718 (2) and LEU844
Complex 9	−8.1	LYS745LYS745LYS87 GLY857 PHE723	2.47818 2.56406 3.79409 3.76916 2.6504	PHE723, LEU718 (2) and LEU844
Complex 10	−8.2	LYS745LYS745ASP855LYS875GLY857	2.499 2.82934 3.37238 3.46133 3.67217	ASP855, LEU844, PHE723, and ALA743
Complex 11	−8.2	LYS745LYS745ASN842LYS875:GLY857	2.49654 2.73608 3.6529 3.53467 3.69398	ASP855, LEU844, PHE723 ALA743, MET790, LEU844, LEU718, and ALA743
Complex	−8.3	LYS745ASP855LYS875GLY857PHE723	2.57602	ASP855, PHE723, LEU718 (2), and LEU844

Table 2 The interactions of the molecules under investigation in the active site of EGFR receptor *(Continued)*

Complex	Binding affinity (Kcal/mol)	H Bond	Bond distance (Å)	Hydrophobic, electrostatic and Other Interactions
12			3.16711 3.67089 3.72071 2.58988	
Complex 13	−8.3	LYS745LYS745ASP855GLY857	2.55105 2.7272 3.26506 3.67378	ASP855, LEU718, PHE723, LEU718, LEU792, MET793, LEU844, LEU844
Complex 14	−8.3	LYS745GLY796GLY857PHE723	2.5629 3.44018 3.67278 2.64954	ASP855, LEU718 (2), PHE723 and LEU844
Complex 15	−8.4	LYS745ASP855LYS875GLY79 GLY857 PHE723	2.61401 3.24347 3.63358 3.41857 3.69224 2.56581	ASP855, PHE723, LEU718 (2), and LEU844
Complex 16	−7.0	ASP855LYS745GLY857	2.56743 2.30238 3.46178	ASP855, PHE723, LEU718, and VAL726
Complex 17	−9.7	MET790LYS745ASN842ASP855GLY857PHE723	2.57246 2.57583 3.57065 3.30557 3.70673 2.6945	ASP855, PHE723, LEU718 (3), LEU792, and LEU844
Complex 18	−9.0	MET790ASP855LYS745LYS745ASP855LYS875GLY857	2.78194 2.60096 2.56118 2.63813 3.35712 3.54465 3.735	ASP855, PHE723, LEU718, and LEU844
Complex 19	−9.5	MET790LYS745ASP837ASP855GLY857PHE723	2.59334 2.64227 3.57828 3.31602 3.68944 2.673	ASP855, A:LEU718 (3), PHE723, LEU792, and LEU844
Complex 20	−9.0	LYS745LYS745ASP837GLY857	2.48189 2.7112 3.54803 3.65017	ASP855, PHE723, LEU718 (2), and LEU844
Complex 21	−8.4	ASP855LYS745LYS745ASP855 LYS875GLY857	2.90321 2.46076 2.66728 3.2402 3.48286 3.7513	ASP855, MET790, PHE723, LEU718 (2), ALA743, and LEU844 (2)
Complex 22	−9.8	MET790LYS745ASP855GLY857PHE723	2.64611 2.67379 3.20518 3.69658 2.62473	ASP855,LEU844, MET790, PHE723, LEU718 (3), ALA743, and LEU844
Complex 23	−8.8	LYS745GLY796ASP800	2.48434 2.7674 3.71611	LYS745, ASP855, MET790, VAL726, LEU844, LEU718, CYS797, and PHE723
Complex 24	−9.7	LYS745ASN842GLY857PHE723	2.57931 3.47241 3.71569	ASP855, LEU844 (2), MET790, PHE723, LEU718 (3),VAL726, and ALA743

Table 2 The interactions of the molecules under investigation in the active site of EGFR receptor *(Continued)*

Complex	Binding affinity (Kcal/mol)	H Bond	Bond distance (Å)	Hydrophobic, electrostatic and Other Interactions
			2.53735	
Complex 25	−9.3	LYS745ASP837GLY857PHE723	2.47544 3.56847 3.68984 2.69826	ASP855, LEU718(2), LEU844 (2), MET790, PHE723, VAL726, ALA743
Complex 26	−7.9	LYS745ARG841ASP837GLY857	2.72291 2.36452 3.7322 3.53516	ASP855, LEU718, VAL726, ALA743, and LEU844
Complex 27	−7.6	ASP855MET793	2.60582 3.54353	PHE723 and LEU858
Complex 28	−8.1	ASP855	2.80197	ASP855, PHE723, and LEU858

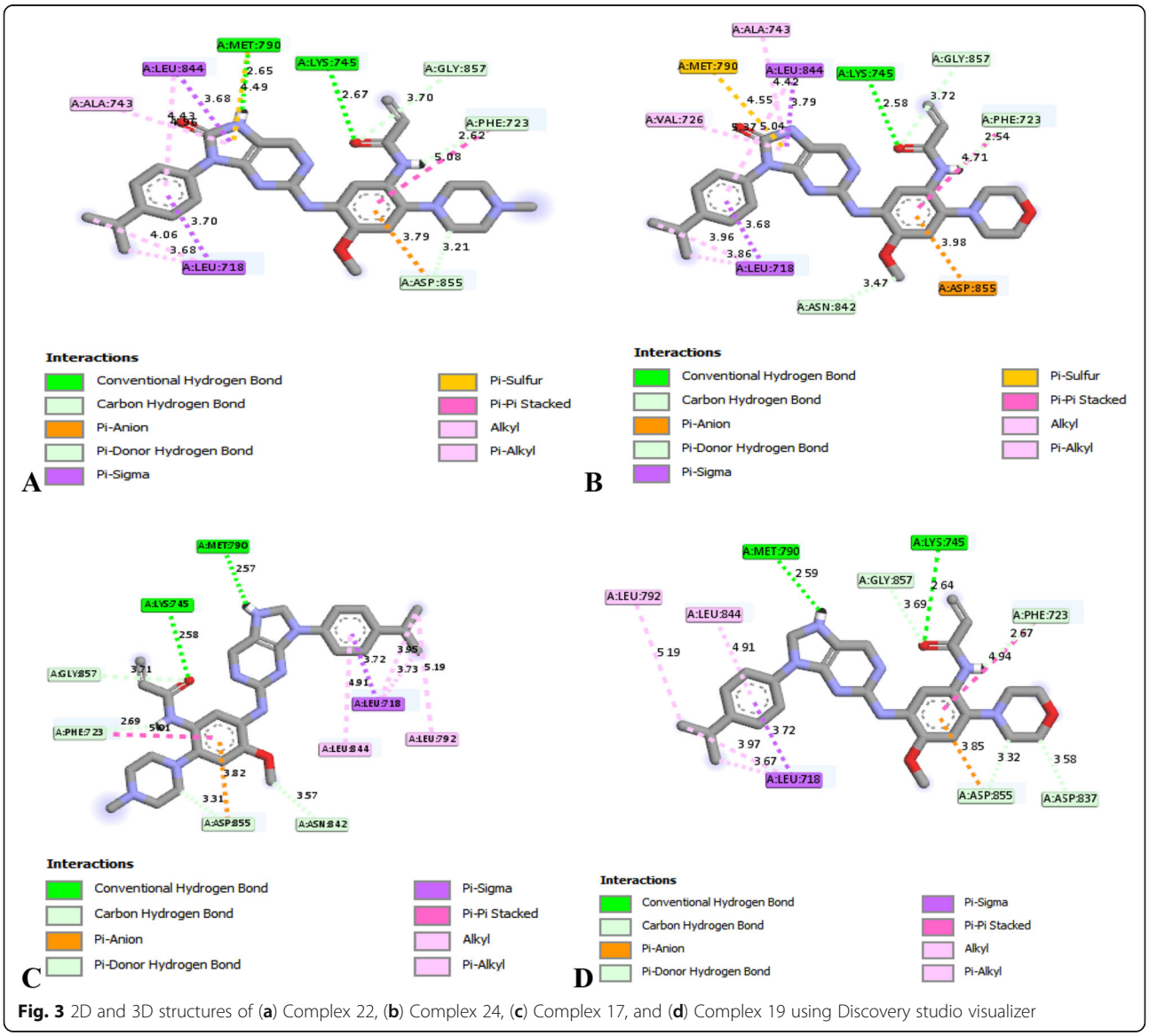

Fig. 3 2D and 3D structures of (**a**) Complex 22, (**b**) Complex 24, (**c**) Complex 17, and (**d**) Complex 19 using Discovery studio visualizer

UCSF Chimera, PyMOL, Discovery studio, and SWISSA DME, an online web tool.

Source and sketching of dataset under investigation

Twenty-eight (28) sets of $EGFR^{L858R/T790M}$ inhibitors were gotten from the work of Hu et al. [15] and used in this research. Immediately after the retrieval of the data, the next thing is drawing of all the molecules under investigation in 2D format. Chemdraw software was then used to draw the 2D structures of all the molecules under investigation [16]. Table 1 presents the structures of all the data set under investigation.

Determination of the optimum structures under investigation

Determination of the most stable/optimum geometry of all the molecules on potential energy surface (PES) was achieved by the use of Spartan 14 wave software in this research. B3LYP/6-311G* level of theory with density functional theory (DFT) was used to achieve the searching for the optimum structures under investigation [17].

Ligands, EGFR enzyme preparation and execution of the molecular docking simulation

Ligands preparation is very vital in any molecular docking studies. As such, the preparation of the ligands in this work was done using the optimum geometry of each of the ligands obtained in 2.1 above before the elucidation of their binding interactions and the binding pose of the EGFR enzyme [18]. Figure 1 shows the 3D geometry of a prepared $EGFR^{L858R/T790M}$ inhibitor (ligand) under investigation.

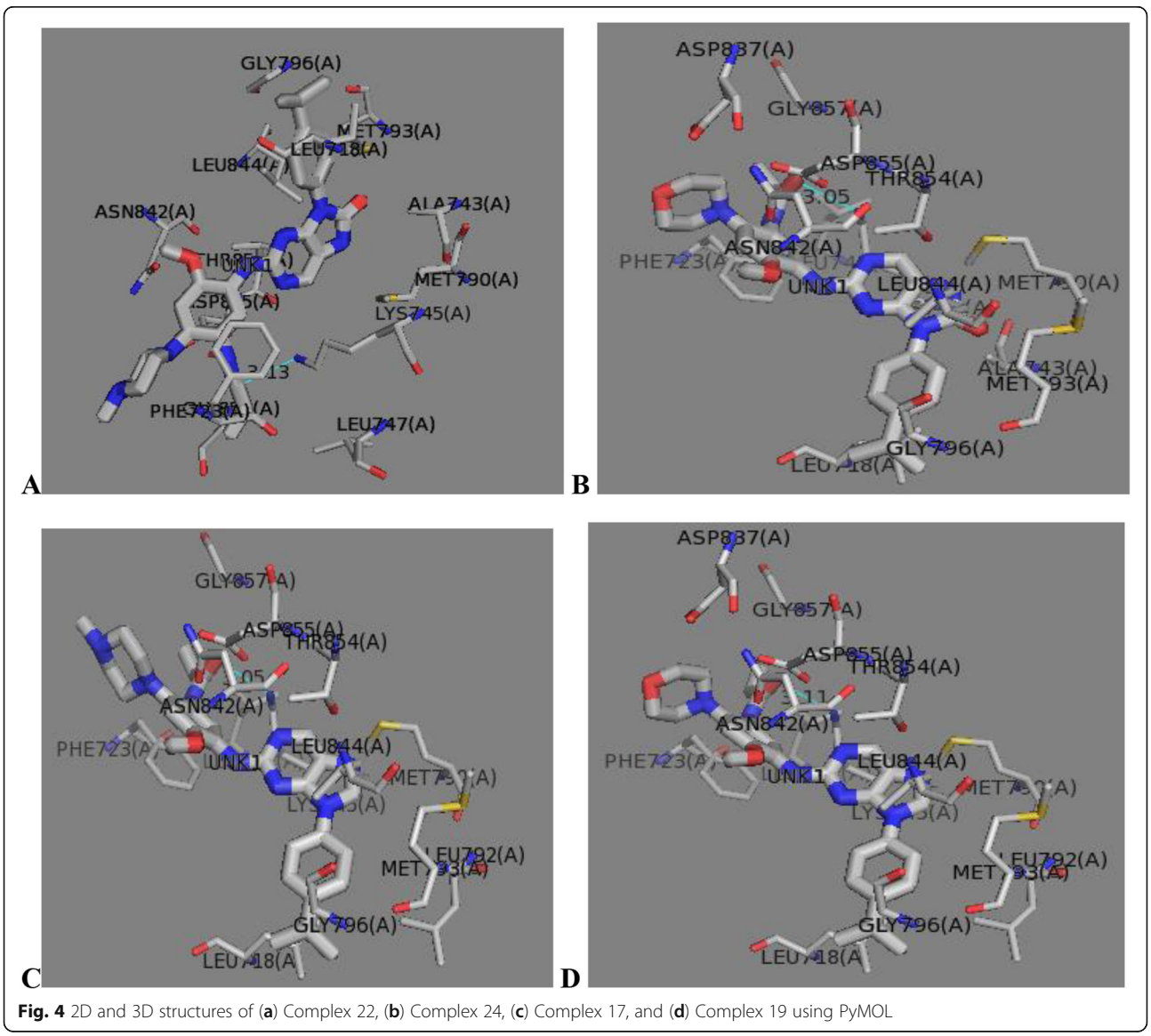

Fig. 4 2D and 3D structures of (**a**) Complex 22, (**b**) Complex 24, (**c**) Complex 17, and (**d**) Complex 19 using PyMOL

The EGFR enzyme with protein data bank code: **3IKA** was retrieved from the RCSB protein data bank database. After successful retrieval of the enzyme, the preparation of the EGFR enzyme for the molecular docking simulation was done using discovery studio visualizer, in the process of the preparation of the enzyme, the co-crystalline ligand and molecule of water present on the structure were deleted. Before that, polar hydrogen was added. Figure 2 shows the 3D structure of the prepared EGFR enzyme.

The docking of the ligands to the binding pose of the EGFR enzyme was achieved with the help of Autodock vina of Pyrex virtual screening software [19]. After a successful docking procedure, since Pyrex was used there is a need to re-couple the docked ligand and the receptor for further investigation. UCSF Chimera software was used for the re-coupling of the docked ligand and the receptor. PyMOL and Discovery studio were used to achieve the visualization of recoupled complexes in order to view the nature of the interaction between the ligand and the receptor.

Drug-likeness and ADME properties prediction

Pharmacokinetics and drug-likeness of the $EGFR^{L858R/T790M}$ inhibitors under investigation were determined using SwissADME, a free online web tool [20]. Lipinski's rule of five was the criteria used in the determination of the drug-likeness of the molecules under investigation which states that if any small molecule violates more than 2 of these criteria, the molecules might not be orally bioavailable [21].

Design

Structure-based drug design is a very robust and useful technique. Structure-based drug design is also called direct design which involves the acquisition of the information regarding the three-dimensional structure of the

Table 3 Pharmacokinetics properties

Molecule	MW	No. of H-bond acceptors	No. of H-bond donors	TPSA	WLOGP	No. of Lipinski's rule violations
Molecule 1	486.57	6	2	100.44	3.5	0
Molecule 2	516.59	7	2	109.67	3.51	1
Molecule 3	500.6	6	2	100.44	3.81	0
Molecule 4	528.65	6	2	100.44	4.62	1
Molecule 5	514.62	6	2	100.44	4.06	1
Molecule 6	504.56	7	2	100.44	4.06	1
Molecule 7	521.01	6	2	100.44	4.15	1
Molecule 8	565.46	6	2	100.44	4.26	1
Molecule 9	612.47	6	2	100.44	4.1	1
Molecule 10	504.56	7	2	100.44	4.06	1
Molecule 11	521.01	6	2	100.44	4.15	1
Molecule 12	565.46	6	2	100.44	4.26	1
Molecule 13	555.46	6	2	100.44	4.81	1
Molecule 14	583.46	7	2	100.44	4.82	1
Molecule 15	539	7	2	100.44	4.71	1
Molecule 16	480.61	6	2	100.44	3.7	0
Molecule 17	526.63	6	2	100.44	3.62	1
Molecule 18	610.45	6	2	100.44	3.1	1
Molecule 19	513.59	6	2	106.43	4.08	1
Molecule 20	597.41	6	2	106.43	3.56	1
Molecule 21	628.46	6	3	120.41	3.4	1
Molecule 22	542.63	6	3	120.41	2.91	1
Molecule 23	626.45	6	3	120.41	2.39	1
Molecule 24	529.59	6	3	126.4	3.37	1
Molecule 25	613.41	6	3	126.4	2.86	1
Molecule 26	515.61	6	3	112.47	3.79	1
Molecule 27	543.66	6	3	112.47	4.83	1
Molecule 28	569.7	6	3	112.47	5.37	1

molecular target (protein) through methods such as x-ray crystallography, NMR spectroscopy, or homology modeling, followed by the design of suitable drug candidates based on the binding affinity and selectivity for their target molecules. Structure-based drug design comprises several steps such as protein structure retrieval and preparation, ligand library preparation, docking and manual design of new compounds [22].

Results

Molecular docking simulation

The results of the molecular docking simulation are presented in Table 2 and Figs. 3 and 4 respectively.

Drug-likeness and ADME properties prediction

The results of the drug-likeness and ADME properties prediction are presented in Tables 3 and 4, Figs. 5 and 6 respectively.

Molecular docking of designed compounds

The results of the molecular docking of designed compounds are presented in Tables 5 and 6 and Fig. 7 respectively.

Drug-likeness and ADME properties prediction

The result of the drug-likeness and ADME properties prediction **is** presented in Tables 7 and 8, respectively.

Discussion

Molecular docking simulation

Molecular docking simulation was used to screen twenty-eight (28) sets of $EGFR^{L858R/T790M}$ inhibitors in order to identify hit compounds that could be used to design new $EGFR^{L858R/T790M}$ inhibitors by investigating their binding interactions in the binding pose of EGFR receptor (**3IKA**) (Table 2). The result of the four best hit

Table 4 Boiled-egg and CYP isoforms inhibition

Molecule	GI absorption	BBB permeant	Pgp substrate	CYP1A2 inhibitor	CYP2C19 inhibitor	CYP2C9 inhibitor	CYP2D6 inhibitor	CYP3A4 inhibitor
Molecule 1	High	No	Yes	No	Yes	Yes	Yes	Yes
Molecule 2	High	No	Yes	No	Yes	Yes	Yes	Yes
Molecule 3	High	No	No	No	Yes	Yes	Yes	Yes
Molecule 4	High	No	No	No	Yes	Yes	Yes	Yes
Molecule 5	High	No	No	No	Yes	Yes	Yes	Yes
Molecule 6	High	No	Yes	No	Yes	Yes	Yes	Yes
Molecule 7	High	No	No	No	Yes	Yes	Yes	Yes
Molecule 8	High	No	No	No	Yes	Yes	Yes	Yes
Molecule 9	High	No	No	No	Yes	Yes	Yes	Yes
Molecule 10	High	No	Yes	No	Yes	Yes	Yes	Yes
Molecule 11	High	No	No	No	Yes	Yes	Yes	Yes
Molecule 12	High	No	No	No	Yes	Yes	Yes	Yes
Molecule 13	High	No	No	No	Yes	Yes	Yes	Yes
Molecule 14	High	No	No	No	Yes	Yes	Yes	Yes
Molecule 15	High	No	No	No	Yes	Yes	Yes	Yes
Molecule 16	High	No	No	No	Yes	Yes	Yes	Yes
Molecule 17	High	No	Yes	No	Yes	Yes	Yes	Yes
Molecule 18	High	No	Yes	No	Yes	Yes	Yes	Yes
Molecule 19	High	No	Yes	No	Yes	Yes	Yes	Yes
Molecule 20	High	No	Yes	No	Yes	Yes	Yes	Yes
Molecule 21	High	No	Yes	No	Yes	Yes	Yes	Yes
Molecule 22	High	No	Yes	No	Yes	Yes	Yes	Yes
Molecule 23	High	No	Yes	No	Yes	Yes	Yes	Yes
Molecule 24	High	No	Yes	No	Yes	Yes	Yes	Yes
Molecule 25	High	No	Yes	No	Yes	Yes	Yes	Yes
Molecule 26	High	No	Yes	No	Yes	Yes	Yes	Yes
Molecule 27	High	No	No	No	Yes	Yes	Yes	Yes
Molecule 28	Low	No	Yes	No	Yes	Yes	Yes	Yes

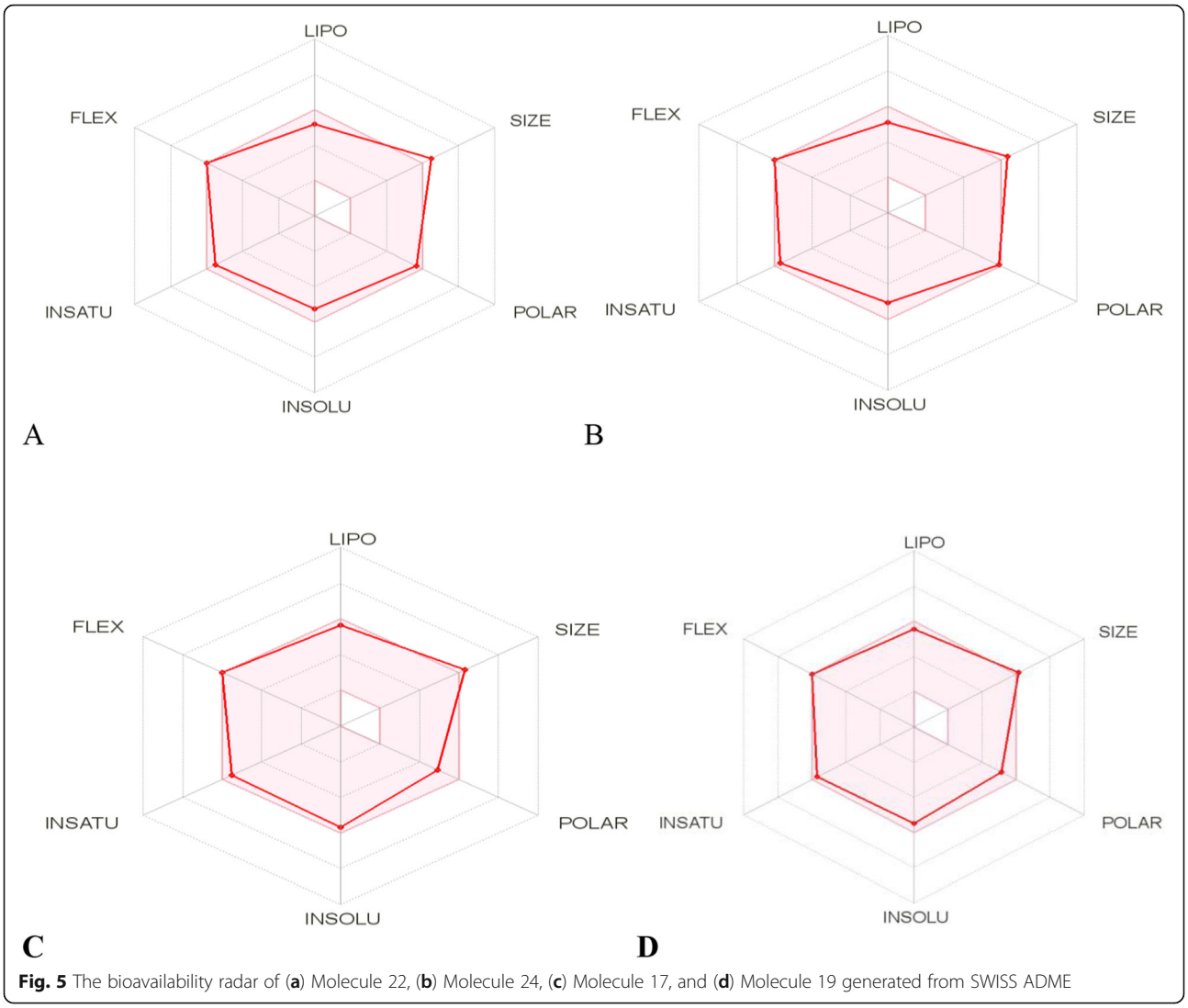

Fig. 5 The bioavailability radar of (**a**) Molecule 22, (**b**) Molecule 24, (**c**) Molecule 17, and (**d**) Molecule 19 generated from SWISS ADME

compounds with the lowest docking scores/highest binding affinity will be discussed.

Compound 22 was the best among the four selected compounds that have the lowest docking score of −9.8 kcal/mol due to the major number of interactions in the binding pocket of the enzyme. Discovery studio visualizer was used to investigate its interaction in the binding pose of the enzyme, it was seen to interact with MET790 (2.65 Å), LYS745 (2.67 Å), ASP855 (3.21 Å), GLY857 (3.69 Å) and PHE723 (2.63 Å) amino acid residues in the active site of EGFR receptor via both conventional and carbon-hydrogen bond interactions. Beside conventional and carbon-hydrogen bond interactions, it also bound to LEU844, PHE723, LEU718 (3), ALA743, and LEU844 residues via Pi-Sigma, Pi-Sulfur, Pi-Pi Stacked, Alkyl, and Pi-Alkyl hydrophobic interactions. Pi-Anion electrostatic interaction with ASP855 and Pi-Sulfur interaction with MET790 were also observed.

The second best with a binding affinity of −9.7 kcal/mol was compound 24. It bound with LYS745 (2.58 Å), ASN842 (3.47 Å), GLY857 (3.72 Å), and PHE723 (2.54 Å) residues in the binding pose of the receptor through conventional and carbon-hydrogen bond interactions. Pi-Sigma, Pi-Pi Stacked, Alkyl, and Pi-Alkyl hydrophobic interactions were also observed with ASP855, LEU844 (2), PHE723, LEU718 (3), VAL726, and ALA743 residues. Apart from the interaction mentioned, Pi-Anion electrostatic interaction with ASP855 and Pi-Sulfur interaction with MET790 amino acid residues respectively were also seen.

The third best in the trend is compound 17 which also found to bound *via* conventional and carbon-hydrogen bond interactions with MET790 (2.57 Å), LYS745 (2.58 Å), ASN842 (3.57 Å), ASP855 (3.31 Å), GLY857 (3.71 Å), and PHE723 (2.69 Å) amino acid residues respectively. Apart from conventional and carbon-hydrogen bond interactions, it interacted via

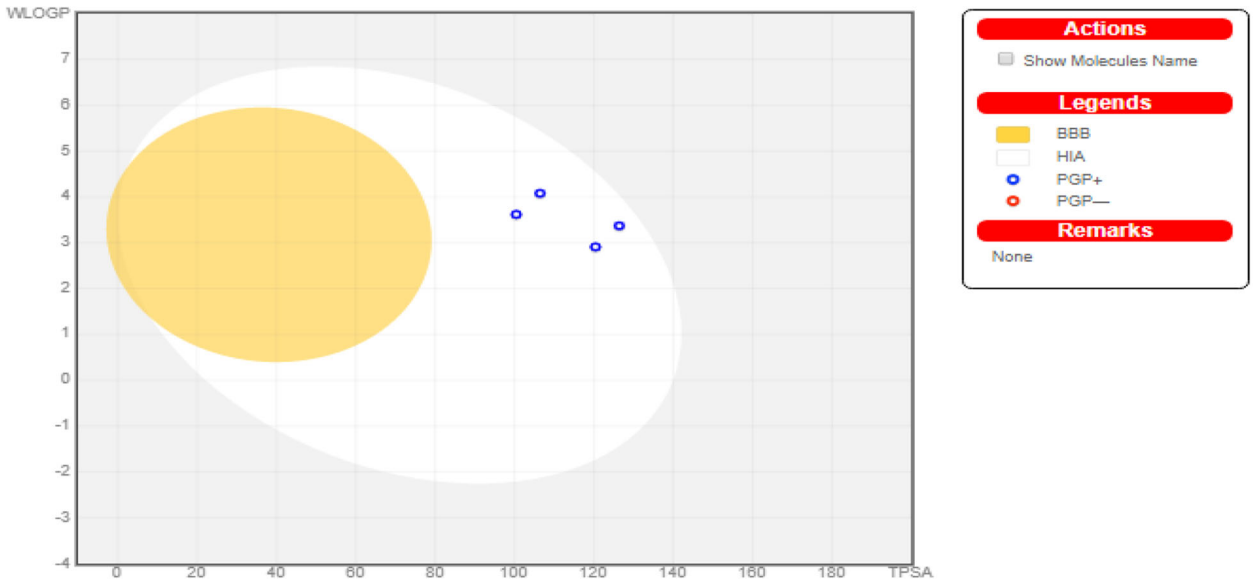

Fig. 6 Boiled-egg Plot of the lead compounds generated from SWISS ADME

Pi-Sigma, Pi-Pi Stacked, Alkyl, and Pi-Alkyl hydrophobic interactions with PHE723, LEU718 (3), LEU792, and LEU844 amino acid residues and also via Pi-Sulfur with MET790 amino acid residue in the binding pose of the receptor. The last one in the trend is compound 19 which also bound with the active site of the receptor *via* conventional and carbon-hydrogen bond interactions, Pi-Sigma, Pi-Pi Stacked, Alkyl, Pi-Alkyl hydrophobic interactions, and Pi-Anion electrostatic interactions as shown in Table 2. Figures 3 and 4 showed the 2D and 3D structures of the four lead compounds investigated using discovery studio visualizer and Pymol.

Drug-likeness and ADME properties prediction of the studied compounds

Table 3 presents the computed drug-likeness of the compounds under investigation. It was observed in the table that none of the molecules under investigation violated more than the maximum permissible limit of the criteria stated by Lipinski's filters, it therefore means that there is a high tendency that all of these molecules might be pharmacologically very active. In fact, all these molecules under investigation are said to have good absorption, low toxicity level, orally bioavailable, and permeable properties except molecule 28 which has WlogP value (it predicts whether a molecule has low toxicity level or not) greater than 5. The Bioavailability Radar of the four selected molecules under investigation was shown to further confirm their drug-likeness properties (Fig. 5). The compounds under investigation could be said to be orally bioavailable.

Table 4 presents the gastrointestinal (GI) absorption, blood-brain barrier (BBB) permeant, Pgp substrate, and CYP isoforms inhibition properties of all the molecules under investigation. From the table, all the molecules under investigation have high GI absorption, none has BBB permeant, some were found to be able to permeate through the skin and some cannot, also all were observed to inhibit the CYP isoforms except CYP1A2. The boiled-egg plot was performed to further confirm the GI absorption and BBB permeant properties of the four hit compounds (Fig. 6). It is further confirmed from the plot that none of them passed through the BBB but they were within the GI absorption region.

Molecular docking of designed compounds

Six new $EGFR^{L858R/T790M}$ inhibitors were designed using compound 22 with the highest binding affinity of −9.8 kcal/mol as the template (Table 5). Based on the interaction of compound 22 with the EGFR receptor, structural modifications were carried out on the template by the addition of substituents on the piperazin-1-yl moiety and isopropyl phenyl ring of the template.

The addition of acetyl group on the piperazin-1-yl moiety and 2 chlorine molecules at the meta position of the isopropyl phenyl ring of the template showed a significant increase in the interaction of the designed compound (D3) with the EGFR receptor with −10.2 kcal/mol binding energy. It was found to bind with the EGFR receptor through conventional and carbon-hydrogen bonds, hydrophobic, electrostatic, and other interactions (Table 6). Four amino acid residues (ASP855, MET790, LYS745, and LYS745) of the enzyme with bond distance 2.9622 Å, 2.49526 Å, 2.61911 Å, and 2.38759 Å were

Table 5 The designed compounds with their binding affinities

S/NO	Structures	Docking scores (kcal/mol)
D1	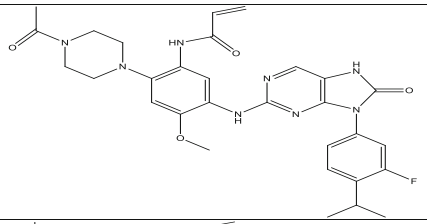	-10
D2	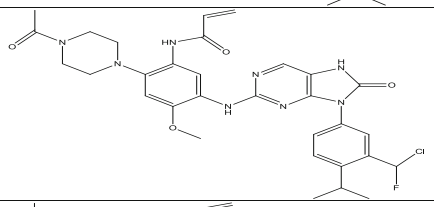	-10
D3	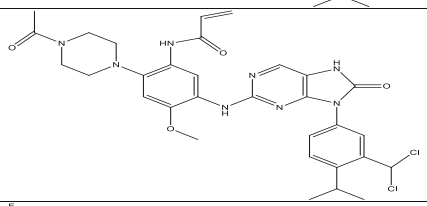	-10.2
D4	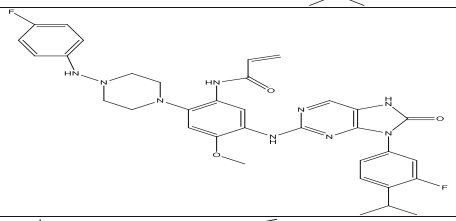	-9.9
D5	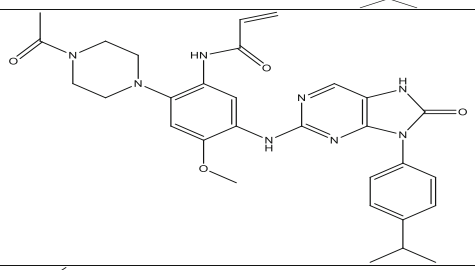	-10.1
D6	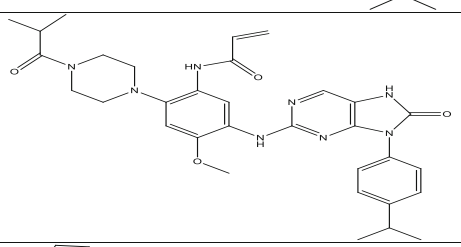	-10
AZD9291	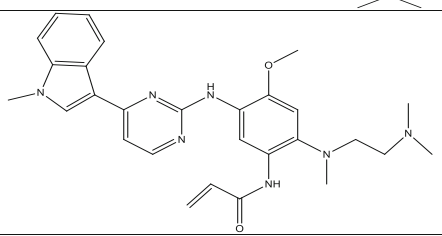	-8.1

Template Compound 6 (Binding energy = -9.8)

Template Compound 6 (binding energy = −9.8)

Table 6 The interactions of the designed compounds in the active site of the EGFR receptor

Ligand receptor (3IKA)	Binding energy (kcal/mol)	Hydrogen bond	Bond distance (Å)	Hydrophobic and other interactions
1	−10	ASP855, MET790, LYS745, LYS745, ASP855 & PHE723	2.91264, 2.46131, 2.6733, 2.46143, 3.29523 & 2.58927	ASP855, LEU718 (3), MET790, PHE723, LEU792, ALA743 & LEU844 (2)
2	−10	ASP855, MET790, LYS745, ASP855 & PHE723	2.81294, 2.45287, 2.74079, 3.36729 & 2.75797	ASP855, LEU844 (3), MET790, PHE723, LEU718 (4), LEU792, CYS797 & ALA743 (2)
3	−10.2	ASP855, MET790, LYS745, LYS745, ASP855 & PHE723	2.9622, 2.49526, 2.61911, 2.38759, 3.24379 & 2.57647	ASP855, LEU844 (2), MET790, PHE723, LEU718 (3), LEU792, CYS797 & ALA743 (2)
4	−9.9	ASP855, THR854 & PHE723	2.6829, 2.50494 & 3.54003	ASP855, LEU718, GLY796, PHE723, GLY857, ALA755, LEU747, ILE759, VAL726 & LEU858 (2)
5	−10.1	ASP855, MET790, LYS745, LYS745, ASP855 & PHE723	2.83123, 2.35804, 2.58025, 2.43397, 3.31176 & 2.70789	ASP855, LEU718 (3), MET790, PHE723, LEU792, ALA743 & LEU844 (2)
6	−10	MET790, LYS745, ASP855 & PHE723	2.45034, 2.68227, 3.3187 & 2.46677	ASP855, LEU718 (3), MET790, PHE723, LEU792, LEU858 (2), LYS875 (2), ALA743 & LEU844
AZD9291	−8.1	ASP855, ASP837 & GLY857	2.39196, 3.61636 & 3.55164	MET790, LEU718, VAL726 LEU844 (2) & ALA743 (2)

Template: Compound 22 (binding energy = −9.8)

observed to form a conventional hydrogen bond with a different part of the ligand as depicted in Fig. 7a. Carbon-hydrogen bond was also observed in the binding pocket of the enzyme between these two amino acid residues ASP855 (3.24379 Å) and PHE723 (2.57647 Å) and the ligand. The ten (10) amino acid residues in the binding pocket of the enzyme who interacted with the ligands via hydrophobic interaction were LEU844 (2), MET790, PHE723, LEU718 (3), LEU792, CYS797, and ALA743 (2) respectively. Besides the mentioned interactions, electrostatic interaction was also observed between the ligand (D3) and ASP855 residue in the binding pocket of the receptor. The only amino acid who interacted via Pi-Sulfur interaction (other) was MET790.

The addition of only the acetyl group on the piperazin-1-yl moiety of the template yielded significant change also in the interaction of the designed compound (D5) with the EGFR receptor with a very good binding affinity of −10.1 kcal/mol (Table 5). Designed compound D5 bounded to EGFR receptor via a hydrogen bond, hydrophobic interactions, and other interaction as shown in Table 6. The same number of the conventional

Table 7 Drug-likeness properties of the designed compounds

Molecule	MW	TPSA	WLOGP	No. of H-bond donors	No. of H-bond acceptors	RO5 violations
Molecule 1	588.63	137.48	3.38	3	10	2
Molecule 2	637.1	137.48	4.13	3	11	2
Molecule 3	653.56	137.48	3.98	3	11	2
Molecule 4	655.7	132.44	4.23	4	11	2
Molecule 5	570.64	137.48	2.83	3	6	1
Molecule 6	598.7	137.48	3.46	3	6	1

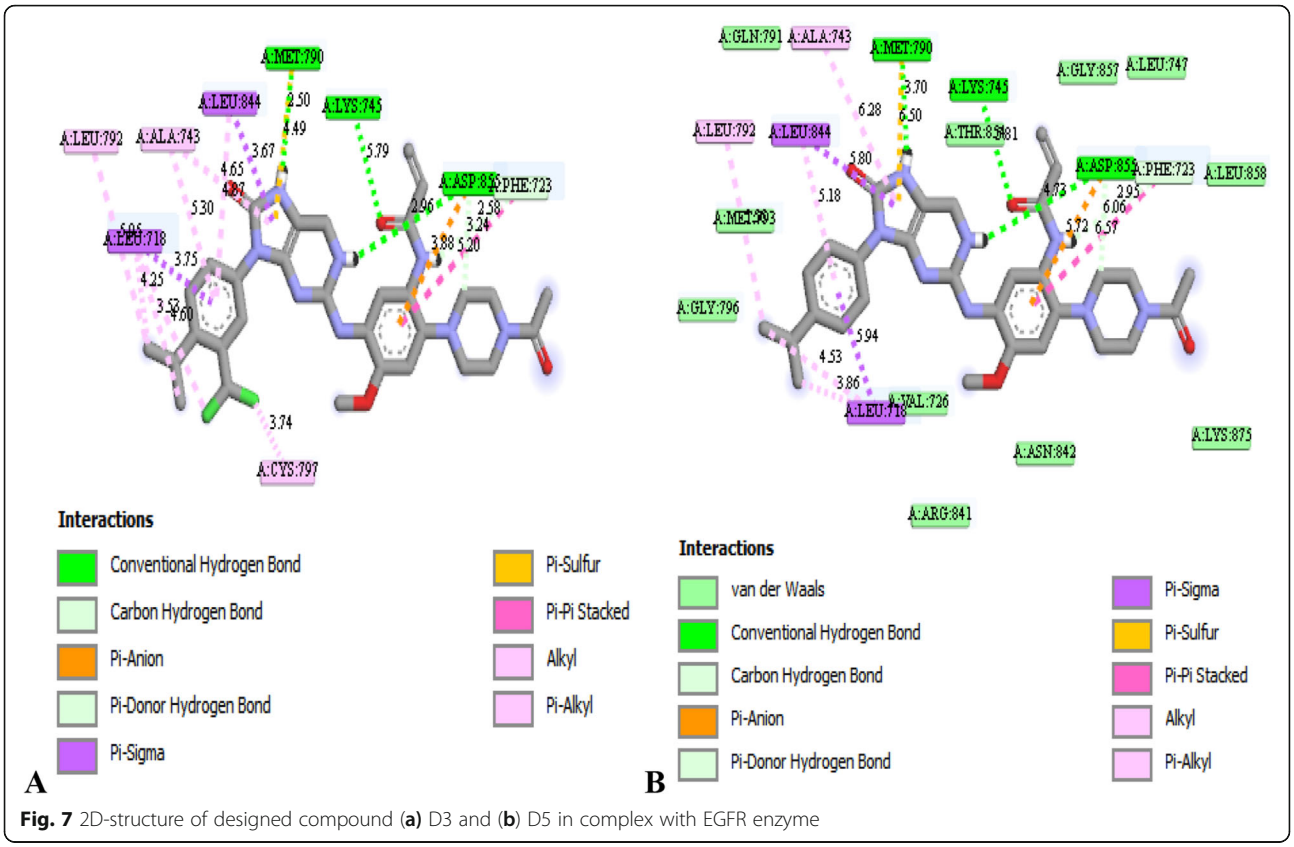

Fig. 7 2D-structure of designed compound (**a**) D3 and (**b**) D5 in complex with EGFR enzyme

hydrogen bond, carbon-hydrogen bond, electrostatic, and Pi-Sulfur (other) interactions were observed between D5 and the receptor except in the hydrophobic interaction where there were eight amino acids which interacted with the ligand. The four amino acid residues with the bond distance that interacted via conventional hydrogen bond with a different part of the ligand as shown in Fig. 7b were ASP855 (2.83123 Å), MET790 (2.35804 Å), LYS745 (2.58025 Å), and LYS745 (2.43397 Å) respectively. The two amino acids that were observed to the carbon-hydrogen bond in the binding pocket of the enzyme and the ligand were ASP855 (3.31176 Å) and PHE723 (2.70789 Å). The eight (8) amino acid residues in the binding pocket of the enzyme which interacted with the ligands via hydrophobic interaction were LEU718 (3), PHE723, LEU792, ALA743, and LEU844 (2) respectively. Besides the mentioned interactions, ASP855 residue was the only that form electrostatic interaction between the ligand and in the binding pocket of the receptor and MET790 was the only residue who interacted via Pi-Sulfur (other) interaction. This might be possible as the result of not having halogens in the designed compound 5 (D5) which is why the number of hydrophobic interactions were less than that of D3.

The other designed compounds (D1, D2, D4, and D6) showed good interactions with higher binding affinity in the binding pocket of the EGFR tyrosine kinase receptor (Table 6). They were observed to have interacted with the binding pocket of the enzyme via the same conventional hydrogen, carbon-hydrogen bond, hydrophobic, electrostatic, and Pi-Sulfur (other) interactions except D4 which has not interacted via

Table 8 ADME Properties of the designed compounds

Molecule	GI absorption	BBB permeant	Pgp substrate	Bioavailability Score	Synthetic Accessibility
Molecule 1	Low	No	Yes	0.17	4.22
Molecule 2	Low	No	Yes	0.17	4.88
Molecule 3	Low	No	No	0.17	4.37
Molecule 4	Low	No	No	0.17	4.68
Molecule 5	Low	No	Yes	0.17	4.17
Molecule 6	Low	No	Yes	0.17	4.4

Pi-Sulfur (other) interaction. Furthermore, AZD9291 was used as a positive control and used to validate the docking process than compared with the designed compounds. The designed compounds were found to be better than AZD9291 which has the binding affinity of −8.1 kcal/mol which is as a result of less number of interactions as compared with the designed compounds. The 2D structures of designed compound D3 and D5 are presented in Fig. 7a and b.

Drug-likeness and ADME prediction of designed compounds

Using the Lipinski's rule of five as a standard filter for small molecule, the drug-likeness of the designed compounds were also predicted as presented in Table 7. From the table, no any designed compound was found to violate more than the permissible limit set by Lipinski's rule of five filters and therefore predicting their easy transportation, absorption, and diffusion [23, 24].

ADME properties of these designed compounds were also predicted and presented in Table 8. All were observed to have low gastrointestinal absorption. But none was observed to permeant through the brain. All designed compounds have a lower bioavailability score of 0.17. Based on the synthetic accessibility score (Table 8), they can all be synthesized in the laboratory [25, 26].

Conclusion

In conclusion, molecular docking simulation carried out on the twenty-eight (28) $EGFR^{L858R/T790M}$ inhibitors has identified four hit compounds with a higher binding affinity toward their target. The hit compounds discovered were compound 22 with −9.8 kcal/mol, 24 with −9.7 kcal/mol, 17 with −9.7 kcal/mol, and 19 with −9.5 kcal/mol respectively. These lead compounds were further subjected to drug-likeness and ADME prediction and found to be orally bioavailable with good absorption, low toxicity level, and permeable properties. The best among the hit compounds was retained as a template and used to design six new $EGFR^{L858R/T790M}$ inhibitors with better binding affinity than the template and AZD9291 (the positive control). None of the designed compounds was found to violate more than the permissible limit set by RO5 thereby predicting their easy transportation, absorption, and diffusion. More so, the designed compounds were found to have good synthetic accessibility which indicates that these designed compounds can be synthesized in the laboratory.

Abbreviations

DFT: Density function theory; B3LYP: Becke's three-parameter read-Yang-Parr hybrid; PDB: Protein data bank; NSCLC: Non-small cell lung cancer agents; EGFR: Epidermal growth factor receptor

Acknowledgements

The authors acknowledge the technical effort of Ahmadu Bello University, Zaria – Nigeria

Authors' contributions

MTI contributed throughout the research work. AU gives directives and technical advice. GAS partake in technical activities. SU also partake in technical activities. All authors have read and approved the manuscript.

Funding

This research did not receive any funding from anybody.

Availability of data and materials

All data and materials are available upon request.

Ethics approval and consent to participate

Not applicable.

Consent for publication

Not applicable.

Competing interests

All authors have declared that there is no conflict of interest regarding this submission.

Received: 5 June 2020 Accepted: 6 August 2020
Published online: 18 August 2020

References

1. Kong L-L, Ma R, Yao M-Y, Yan X-E, Zhu S-J, Zhao P, Yun C-H (2017) Structural pharmacological studies on EGFR T790M/C797S. Biochem Biophys Res Commun 488(2):266–272
2. Song J, Jang S, Lee JW, Jung D, Lee S, Min KH (2019) Click chemistry for improvement in selectivity of quinazoline-based kinase inhibitors for mutant epidermal growth factor receptors. Bioorg Med Chem Lett 29(3):477–480
3. Hanan EJ, Baumgardner M, Bryan MC, Chen Y, Eigenbrot C, Fan P, Gu X-H, La H, Malek S, Purkey HE (2016) 4-Aminoindazolyl-dihydrofuro [3, 4-d] pyrimidines as non-covalent inhibitors of mutant epidermal growth factor receptor tyrosine kinase. Bioorg Med Chem Lett 26(2):534–539
4. Balak MN, Gong Y, Riely GJ, Somwar R, Li AR, Zakowski MF, Chiang A, Yang G, Ouerfelli O, Kris MG (2006) Novel D761Y and common secondary T790M mutations in epidermal growth factor receptor–mutant lung adenocarcinomas with acquired resistance to kinase inhibitors. Clin Cancer Res 12(21):6494–6501
5. Dungo RT, Keating GM (2013) Afatinib: first global approval. Drugs 73(13): 1503–1515
6. Solca F, Dahl G, Zoephel A, Bader G, Sanderson M, Klein C, Kraemer O, Himmelsbach F, Haaksma E, Adolf GR (2012) Target binding properties and cellular activity of afatinib (BIBW 2992), an irreversible ErbB family blocker. J Pharmacol Exp Ther 343(2):342–350
7. Tsao M-S, Sakurada A, Cutz J-C, Zhu C-Q, Kamel-Reid S, Squire J, Lorimer I, Zhang T, Liu N, Daneshmand M (2005) Erlotinib in lung cancer—molecular and clinical predictors of outcome. N Engl J Med 353(2):133–144
8. Cross DA, Ashton SE, Ghiorghiu S, Eberlein C, Nebhan CA, Spitzler PJ, Orme JP, Finlay MRV, Ward RA, Mellor MJ (2014) AZD9291, an irreversible EGFR TKI, overcomes T790M-mediated resistance to EGFR inhibitors in lung cancer. Cancer discovery 4(9):1046–1061
9. Walter AO, Sjin RTT, Haringsma HJ, Ohashi K, Sun J, Lee K, Dubrovskiy A, Labenski M, Zhu Z, Wang Z (2013) Discovery of a mutant-selective covalent inhibitor of EGFR that overcomes T790M-mediated resistance in NSCLC. Cancer discovery 3(12):1404–1415
10. Park, K., J.-S. Lee, K.H. Lee, J.-H. Kim, B.C. Cho, Y.J. Min, J.Y. Cho, J.-Y. Han, B.-S. Kim, and J.-S. Kim, (2016), Olmutinib (BI 1482694; HM61713), an EGFR mutant-specific inhibitor, in T790M+ NSCLC: efficacy and safety at the RP2D, J Clin Oncol, 34 (suppl), abstr 9055.
11. Paz-Ares L, Tan E-H, O'byrne K, Zhang L, Hirsh V, Boyer M, Yang J-H, Mok T, Lee K, Lu S (2017) Afatinib versus gefitinib in patients with EGFR mutation-positive advanced non-small-cell lung cancer: overall survival data from the phase IIb LUX-Lung 7 trial. Ann Oncol 28(2):270–277
12. Song Z, Ge Y, Wang C, Huang S, Shu X, Liu K, Zhou Y, Ma X (2016) Challenges and perspectives on the development of small-molecule EGFR

inhibitors against T790M-mediated resistance in non-small-cell lung cancer: miniperspective. J Med Chem 59(14):6580–6594
13. Beheshti A, Pourbasheer E, Nekoei M, Vahdani S (2016) QSAR modeling of antimalarial activity of urea derivatives using genetic algorithm–multiple linear regressions. Journal of Saudi Chemical Society 20(3):282–290
14. Khan, M.F., G. Verma, W. Akhtar, M. Shaquiquzzaman, M. Akhter, M.A. Rizvi, and M.M. Alam, (2016), Pharmacophore modeling, 3D-QSAR, docking study and ADME prediction of acyl 1, 3, 4-thiadiazole amides and sulfonamides as antitubulin agents, Arabian Journal of Chemistry,
15. Hu J, Han Y, Wang J, Liu Y, Zhao Y, Liu Y, Gong P (2018) Discovery of selective EGFR modulator to inhibit L858R/T790M double mutants bearing a N-9-Diphenyl-9H-purin-2-amine scaffold. Bioorg Med Chem 26(8):1810–1822
16. Ibrahim MT, Uzairu A, Shallangwa GA, Ibrahim A (2018) Computational studies of some biscoumarin and biscoumarin thiourea derivatives ASα-GLUCOSIDASE INHIBITORS. The Journal of Engineering and Exact Sciences 4(2):0276–0285
17. Kohn W, Becke AD, Parr RG (1996) Density functional theory of electronic structure. J Phys Chem 100(31):12974–12980
18. Adeniji, S.E., S. Uba, and A. Uzairu, (2018), Quantitative structure-activity relationship and molecular docking of 4-Alkoxy-Cinnamic analogues as anti-mycobacterium tuberculosis, Journal of King Saud University-Science,
19. Ibrahim, M.T., A. Uzairu, G.A. Shallangwa, and A. Ibrahim, (2018), In-silico studies of some oxadiazoles derivatives as anti-diabetic compounds, Journal of King Saud University-Science,
20. Daina A, Michielin O, Zoete V (2017) SwissADME: a free web tool to evaluate pharmacokinetics, drug-likeness and medicinal chemistry friendliness of small molecules. Sci Rep 7:42717
21. Ismail, S.Y., A. Uzairu, B. Sagagi, and M. Sabiu, (2018), In silico molecular docking and pharmacokinetic study of selected phytochemicals with estrogen and progesterone receptors as anticancer agent for breast cancer, 5 (3), 1337-1350.
22. Batool M, Ahmad B, Choi S (2019) A structure-based drug discovery paradigm. Int J Mol Sci 20(11):2783
23. Ibrahim MT, Uzairu A, Shallangwa GA, Uba S (2020) Computer-aided molecular modeling studies of some 2, 3-dihydro-[1, 4] dioxino [2, 3-f] quinazoline derivatives as EGFR WT inhibitors. Beni-Suef University Journal of Basic and Applied Sciences 9:1–10
24. Khan I, Garikapati KR, Setti A, Shaik AB, Makani VKK, Shareef MA, Rajpurohit H, Vangara N, Pal-Bhadra M, Kamal A (2019) Design, synthesis, in silico pharmacokinetics prediction and biological evaluation of 1, 4-dihydroindeno [1, 2-c] pyrazole chalcone as EGFR/Akt pathway inhibitors. Eur J Med Chem 163:636–648
25. Ibrahim MT, Uzairu A, Shallangwa GA, Uba S (2020) In-silico activity prediction and docking studies of some 2, 9-disubstituted 8-phenylthio/phenylsulfinyl-9 h-purine derivatives as Anti-proliferative agents. Heliyon 6(1):e03158
26. Hosen S, Dash R, Khatun M, Akter R, Bhuiyan MHR, Rezaul M, Karim NJM, Ahamed F, Islam KS, Afrin S (2017) In silico ADME/T and 3D QSAR analysis of KDR inhibitors. Journal of Applied Pharmaceutical Science 7(01):120–128

Publisher's Note